CHAPTER 5

DESIGN OF BLU-RAY DVD-BASED SERS SUBSTRATE FOR DETECTION AND ANALYSIS OF ROTAVIRUS RNA

Detection of biomolecular samples is often required in research and clinical laboratory applications. Present chapter demonstrates the functioning of a SERS substrate that has been obtained by drop-casting of AuNPs on a bare Blu-ray digital versatile disc (BR-DVD) substrate. The performance of the proposed SERS substrate has been initially evaluated with standard Raman active samples, malachite green (MG) and 1,2-bis(4-pyridyl)ethylene (BPE). The designed SERS substrate yields an average enhancement factor (EF_{avg}) 3.2×10^6 while maintaining a reproducibility characteristics as good as 94% over the sensing region of the substrate. The usability of the SERS substrate has been demonstrated through the detection and analysis of purified rotavirus double-stranded RNA (dsRNA) samples in the laboratory environment condition.

5.1 Introduction

Due to the high sensitivity with unique fingerprinting capability, SERS-based analytical techniques have been extensively used to analyse biological samples. Nucleic acid analysis based on SERS encoded nanoparticles, SERS-based DNA and RNA analyses have been reported in recent years. These studies help to understand various compositions of RNAs and DNAs of different biological samples. Quantitative detection of RNAs and DNAs using SERS-based techniques is challenging because of the low reproducibility of the spectra.

In this chapter, a relatively simple and low-cost platform to develop SERS substrates for the detection and analysis of rotavirus RNA sample in the laboratory environment is demonstrated. The proposed SERS substrate has been fabricated through decorating AuNPs of average dimension 23 nm over the nanochannels of bare BR-DVD substrate. The nanochannels of commercially available BR-DVD are of width 100 nm and channel depth 20 nm [1]. Such structures are ideal for trapping metal nanoparti-

cles of average dimension less than 100 nm while effective in producing guided-mode resonance (GMR) field by the polycarbonate channels of the BR-DVD substrate [2]. For the designed SERS substrate, the combined effect of the hot-spot region and the GMR field enhances the intensities of the scattered Raman signals from the analyte samples when irradiated with a laser source. The usability of the proposed SERS substrate has been realized through detection and analysis of rotavirus dsRNA. With the designed BR-DVD SERS substrate, rotavirus dsRNA concentration as low as 10 ng/µL could be detected with a reproducibility as good as 94% over the sensing region of the substrates. Figure 5.1 represents the schematic representation of the proposed SERS sensing setup.

5.2 Materials and methods

5.2.1 Materials

Blu-ray Disc from SONY Inc. has been procured from an online shopping store. Gold chloride trihydrate ($HAuCl_4 \cdot 3H_2O$) was procured from Himedia, India. Trisodium citrate dihydrate ($C_6H_5Na_3O_7 \cdot 2H_2O$) has been purchased from Merck, India. The Raman active samples, MG and BPE ($C_{12}H_{12}N_2$) were procured from Thermo Fisher Scientific and Sigma-Aldrich, respectively. Commercial SERS substrate has been acquired from SERSitive Inc., Warsaw, Poland. All chemicals were utilized as supplied without additional processing and deionized (DI) water was employed to prepare all experimental samples.

5.2.2 RNA extraction from rotavirus

The clinical diarrheal stool samples were primarily screened to detect the presence of rotavirus antigen through following the standard protocol from the Premier Rotaclone® solid-phase sandwitch enzyme immunoassay (Meridian Bioscience, Cincinnati, Ohio) [3]. The fecal samples were diluted with sterile 1X phosphate-buffered saline (PBS) to prepare 20% viral suspension and clarified by centrifugation at 12000 rpm for 12 minutes at 4°C, and then filtered using a 0.22 µm syringe filter. Subsequently, total RNA has been extracted from 20% stool suspension filtrated by TRIzol method using TRIzol^{TM} Reagent (Invitrogen^{TM}; Cat. No. 15596018) following the manufacturer's protocol [4]. Figure 5.2 depicts the flowchart of the procedure of extracting rotavirus RNA from the clinical stool specimen.

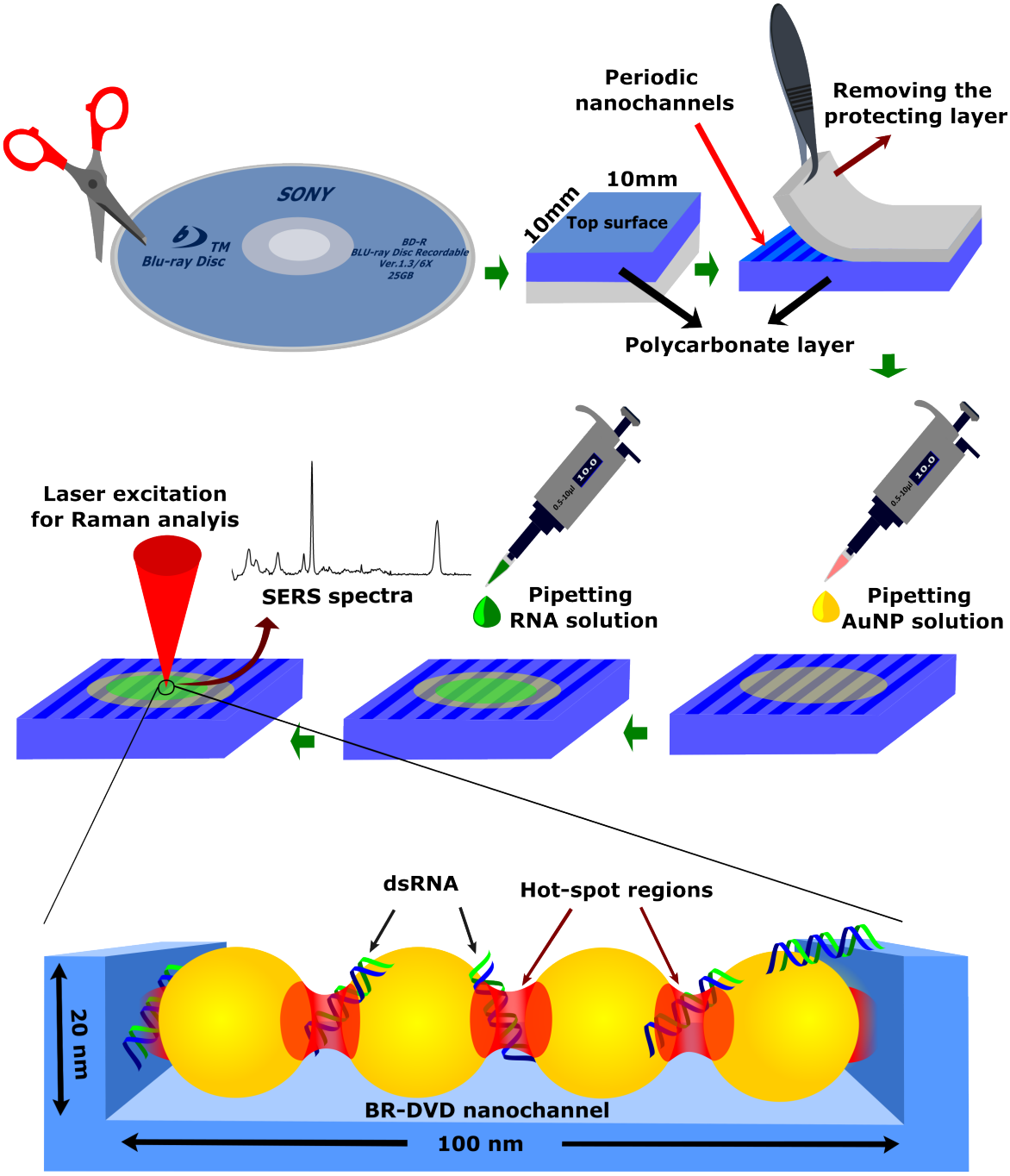

Figure 5.1: Schematic representation of the experimental procedure starting from cutting the BR-DVD into several pieces for the collection of the SERS signal. Schematic also shows the generation of localized electromagnetic fields by the AuNPs trapped into the BR-DVD nanochannels and the generation of highly enhanced SERS spectra of RNAs.

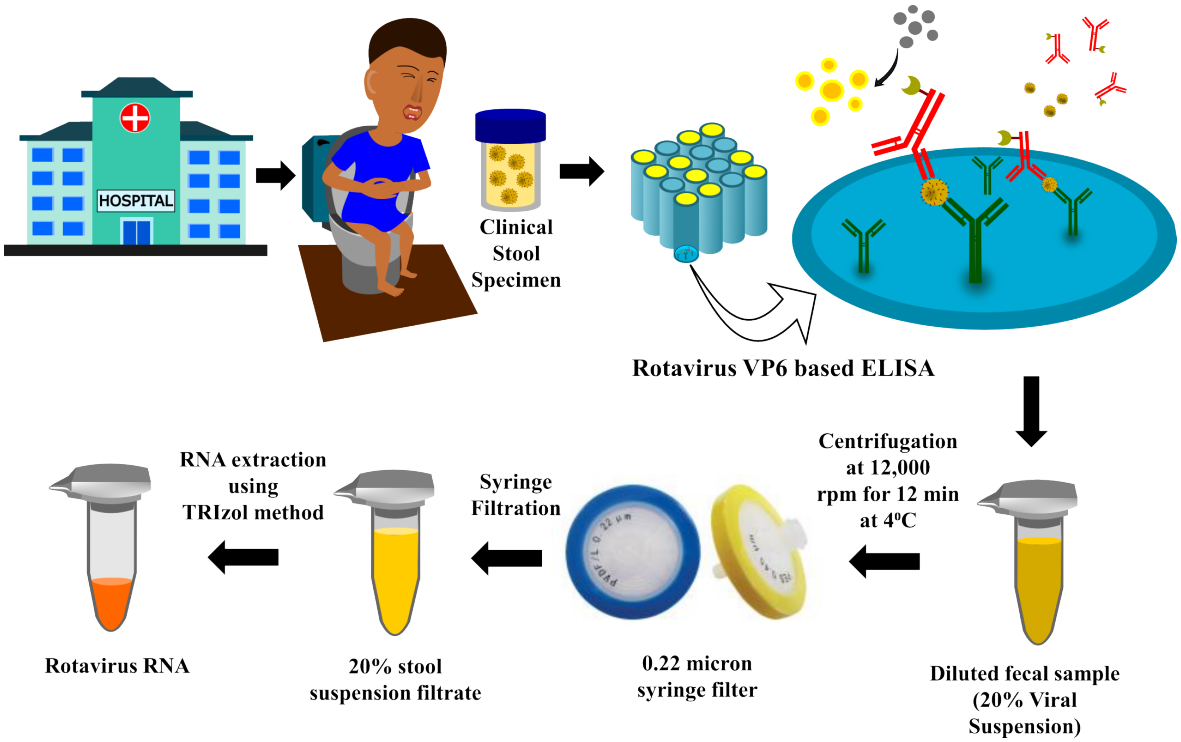

Figure 5.2: Flowchart showing the procedure of extracting rotavirus RNA from clinical stool specimens.

5.2.3 Electromagnetic simulation study

To estimate the magnitude of the LSPR field due to the trapping of the AuNPs in the nanochannels of BR-DVD, simulation study using COMSOL Multiphysics software has been performed. This specific simulation is based on finite element method, where the domain is considered to be composed of infinitesimally small meshes and the net electromagnetic enhancement is estimated by calculating the field in each mesh and integrating it over the whole domain. The physical domain here contains the nanoparticles, an air medium of thickness of 500 nm, and a polycarbonate substrate of thickness of 300 nm. The nanoparticles are placed on the surface of the polycarbonate substrate which is considered as x-y plane. Linearly polarized laser light is allowed to incident along the positive z-axis on the nanoparticles. A 200 nm thick perfectly matched layer (PML) is added outside the physical domain to absorb the scattered light. Laser light of wavelengths 785 nm and intensity of 5×10^8 Wm^{-2} has been considered for the simulation study. To replicate the BR-DVD nanostructure in the simulation, a nanochannel of structural periodicity of 320 nm with a channel width of 100 nm and channel depth 20 nm has been added inside of which nanoparticles are being trapped. Figure 5.3(a) shows the TEM image of the synthesized AuNPs. The average diameter of the AuNPs are estimated to be 23 nm. For the present simulation work, AuNPs of average dimension 20 nm has been considered that were trapped in the nanochannel of the BR-DVD substrate. Prior to evaluate the intensity of the coupled

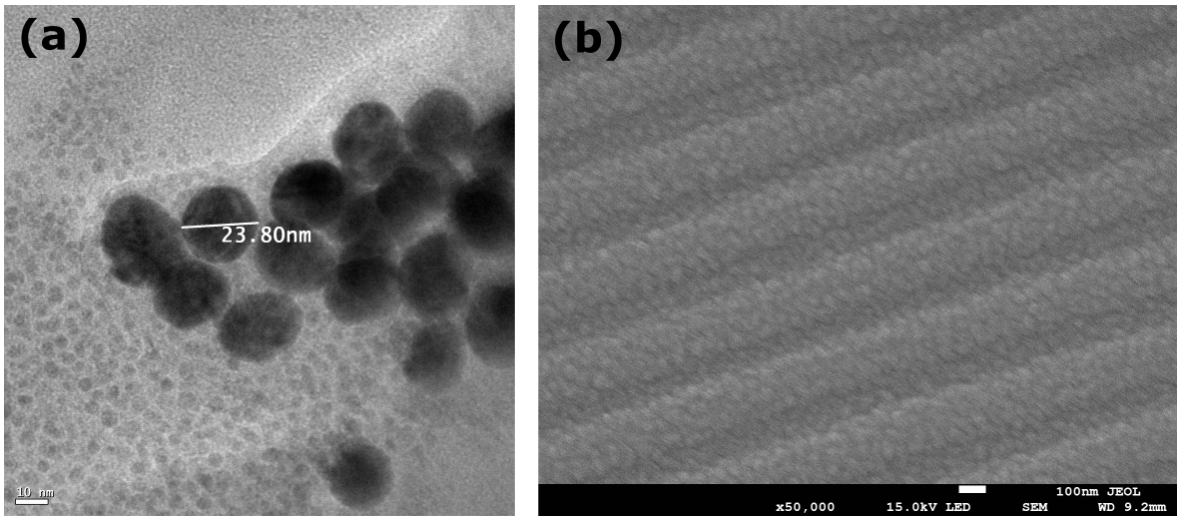

Figure 5.3: (A) TEM image of synthesized AuNPs. (B) FESEM image of bare BRDVD nanochannel surface.

electromagnetic field with the AuNPs trapped in the nanochannels of the BR-DVD substrate, the considered domain has been meshed with proper mesh elements. The physical domain and PML domain have been meshed with free tetrahedral and swept mesh elements, respectively [5].

5.2.4 Fabrication of the SERS substrate

AuNPs have been synthesized in the laboratory using the well-known Turkeveich method reported elsewhere [6]. A clean and dry conical flask of volume 250 mL is filled with 100 mL of 0.01 wt% $HAuCl_4 \cdot 3H_2O$ and heated till boiling under vigorous stirring condition. After 15 minutes of boiling, 2.4 mL of 1 wt% $C_6H_5Na_3O_7 \cdot 2H_2O$ has been added to the boiling solution. The colour of the solution gradually turns red, indicating the formation of AuNPs. The synthesized AuNPs are then stored in a refrigerator at 4°C under dark light condition.

Using a scissor, the BR-DVD was cut into small pieces each of dimension 10 mm × 10 mm (Figure 5.1). By using a tweezer, the protecting layer from the BR-DVD was peeled-off to expose the nanochannels. This process is followed by cleaning with ethanol and DI water and drying in a hot air oven for 1 hour. Figure 5.3(b) represents the FESEM image of the bare BR-DVD nanochannel surface having periodic nanostructures where the synthesized AuNPs can be trapped. Upon drying, 10 µL of the synthesized AuNP solution has been pipetted on the BR-DVD substrate and allowed to dry in a vacuum desiccator for 2 hour prior to use it for SERS studies.

5.3 Results and discussions

5.3.1 Electromagnetic simulation

The effect of GMR on the overalle enhancement in the localized electric field magnitude has been studied. In the simulation work, the separation (d) of a single AuNP of diameter 20 nm from the nanochannels is gradually varied from d = 1 nm to d = 10 nm, and the localized electric field amplitudes have been measured upon excitation with 785 nm laser. Figure 5.4(a-f) represent the simulation results of the local electric field variation due to change in separation, d. The localized electric field is more intense in the gap between the AuNP and the BR-DVD nanochannel wall. Figure 5.4(g) shows the plot of the electic field variations with the spacing of the AuNPs from the BR-DVD nanochannels. The electric field gradually decreases with the increase in separation from d = 1 nm to d = 10 nm.

In the next step, two specific orientations of the AuNPs have been considered to estimate the LSPR field magnitude in the nanochannels of the BR-DVD substrate. In the Figure 5.5(a), nanoparticles are oriented along the length of the channel, while in Figure 5.5(b) they are perpendicular to the length of the channel. For both the situations four AuNPs of dimension 20 nm each have been considered in the nanochannels of the BR-DVD substrate. The nanoparticles are further considered to be aligned in the nanochannel of the BR-DVD and spacing between the nanoparticles is considered to be 4 nm. For AuNPs oriented along the length and perpendicular to the length of the BR-DVD nanochannels, the maximum electric field amplitude are found to be 3.9 $\times$ 10^6 Vm^{-1} and 4.65 $\times$ 10^6 Vm^{-1}, respectively when the nanoparticles were illuminated with 785 nm laser source with incident laser power of 0.5 mW. For the designed SERS substrate, the magnitudes of GMR field will depend on the spacing between the AuNPs and the nanochannels of the BR-DVD substrate. The narrower the gap between the channel wall and AuNP, the higher will be the magnitude of the GMR field and vice-versa. This simulation result clearly indicates that the GMR field does contribute to the overall enhancement in the localized electric field magnitude for the designed SERS substrate.

5.3.2 SERS performance of the fabricated substrate

The performance of the designed SERS substrate has been initially evaluated through detecting Raman signals from standard Raman active samples. Two commonly used Raman active samples namely BPE and MG have been considered for the study. 10 µL solutions of BPE and MG each of concentration 1 µM have been pipetted on two separate BR-DVD SERS substrates. Figure 5.6(a) and 5.6(b) represent the characteristic Raman signals of BPE and MG scattered from the BR-DVD SERS substrate as

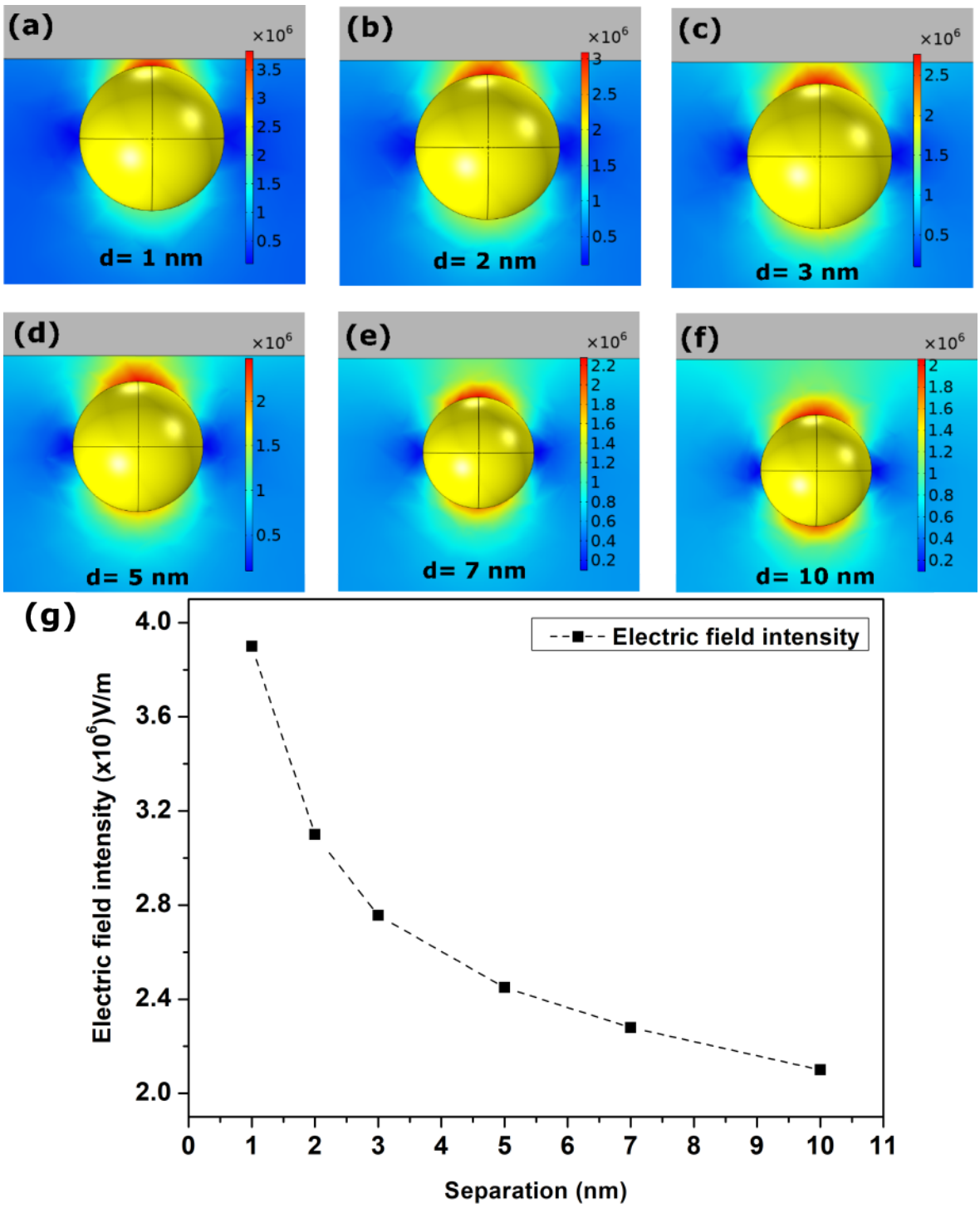

Figure 5.4: (a-f) COMSOL simulation results of the local electric field variation due to change in separation, d of a single AuNP (20 nm diameter) from the wall of the nanochannel. (g) Variation of electric field with the separation of a single AuNP of diameter 20 nm from the nanochannel wall.

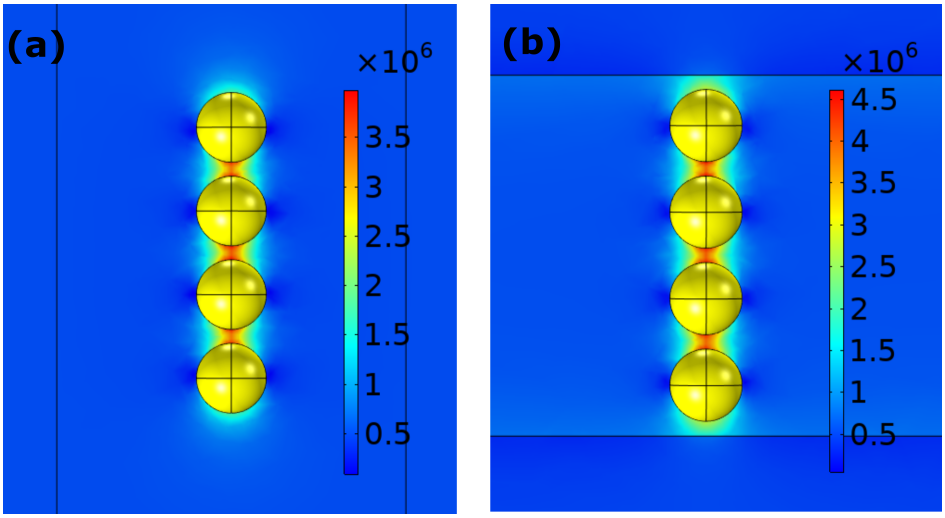

Figure 5.5: COMSOL Multiphysics simulation of four AuNPs of diameter 20 nm each inside the BR-DVD nanochannel, distributed (a) along and (b) perpendicular to the nanochannel excited with a laser of wavelength 785 nm.

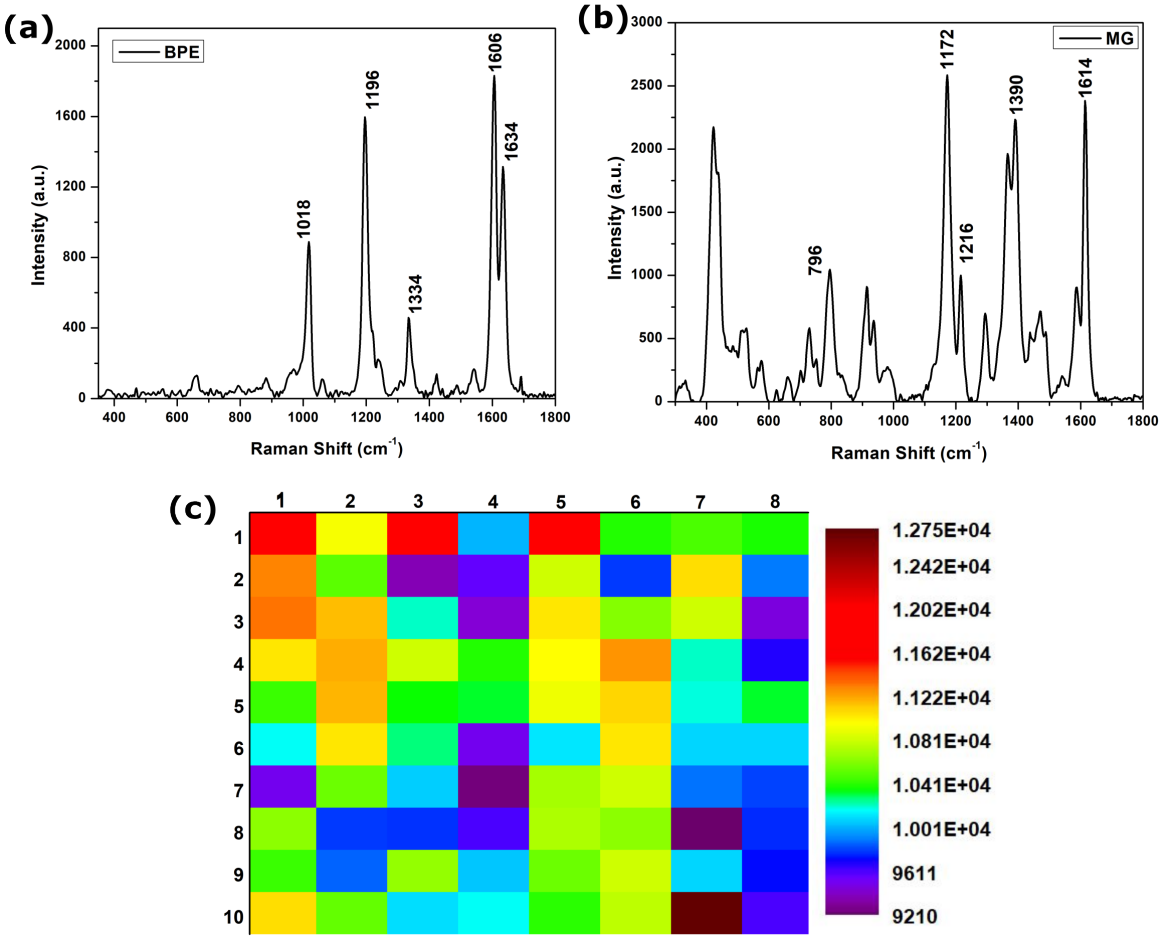

Figure 5.6: SERS spectra of (a) BPE and (b) MG of concentration 1 µM collected from AuNP coated BR-DVD SERS substrate. (c) SERS signal intensity variation of 0.1 mM of MG coresponding to the signature peak at 1172 cm^{-1} over a region 1.6 mm × 2 mm.

recorded by the spectrometer. The characteristic Raman peaks of BPE at 1018 cm^{-1} and 1334 cm^{-1} are attributed to ring breathing and C-H in-plane bending while the peaks at 1196 cm^{-1}, 1606 cm^{-1} and 1634 cm^{-1} are attributed to C-C stretching, C-N bending of the pyridyl ring and C=C stretching, respectively [7–9]. Again the characteristic peaks of MG at 796 cm^{-1}, 1172 cm^{-1}, 1216 cm^{-1}, 1390 cm^{-1} and 1614 cm^{-1} are attributed to ring C-H out of plane bending, ring C-H in-plane vibration, C-H rocking, N-phenyl stretching and ring C-C in-plane stretching vibration, respectively [10–13]. The experimental data further revealed that the SERS spectra of BPE and MG are slightly different from the situation when they considered in powder form [7, 12]. The shift in the Raman peaks is attributed to the orientation of the molecules with the surface of the AuNPs which has caused a distinct SERS spectrum from the situation when the sample is recorded from bare substrate [7, 14].

The EF_{avg} of the developed SERS substrate has been estimated using the following equation as discussed in the section 1.3.3:

$$EF_{avg} = \frac{\frac{I_{SERS}}{N_{SERS}}}{\frac{I_{Raman}}{N_{Raman}}}, \tag{5.1}$$

where, I_{SERS} and I_{Raman} represent SERS and normal Raman scattering intensities, respectively. N_{SERS} and N_{Raman} represents the number of analyte molecules probed for SERS and normal Raman scattering measurements, respectively. First, with MG as a test sample, scattered Raman signal intensity (I_{Raman}) from 10 µL volume of 10 µM MG, pipetted on a bare BR-DVD substrate, was recorded by the Raman spectrometer. After that, 10 µL of 10 nM of the same test sample has been pipetted on the designed BR-DVD SERS substrate and the scattered SERS signal intensity (I_{SERS}) has been recorded. For signature Raman peak of MG at 1172 cm^{-1}, the EF_{avg} has been estimated using equation 5.1 and the value is found to be 3.2×10^6.

Raman spectra from 80 different points over the sensing region of the substrate of dimension 1.6 mm × 2 mm on have been considered. Upon treatment of the substrate with 0.1 mM of MG the signal intensity fluctuations at 1172 cm^{-1} have been recorded. Figure 5.6(c) shows the characteristic mapping of the signature Raman peak intensity variations at 1172 cm^{-1} recorded by the spectrometer. For the considered Raman peak, the maximum variations in the signal intensity was found to be 6%. This infers that the reproducibility of the designed substrate is as good as 94% approximately.

5.3.3 SERS spectra of rotavirus RNA

The usability of the SERS substrate has been realized through monitoring of Raman spectra scattered from rotavirus RNA samples. Characteristic Raman spectrum of this specific RNA sample arises due to the four nucleobases namely- adenine, guanine,

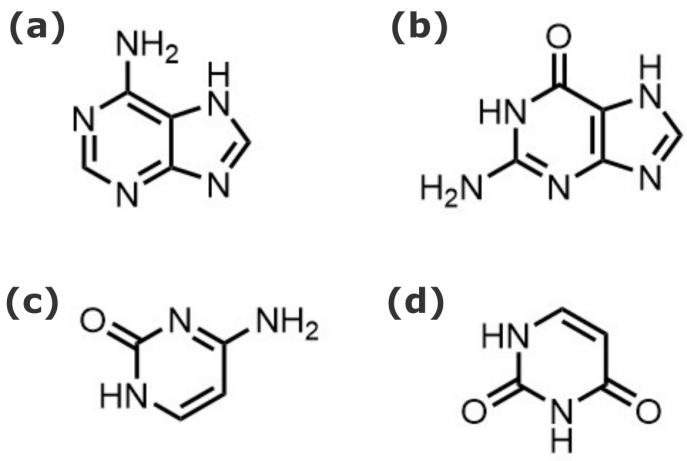

Figure 5.7: Chemical structure of nucleobases (a) adenine, (b) guanine, (c) cytosine and (d) uracil.

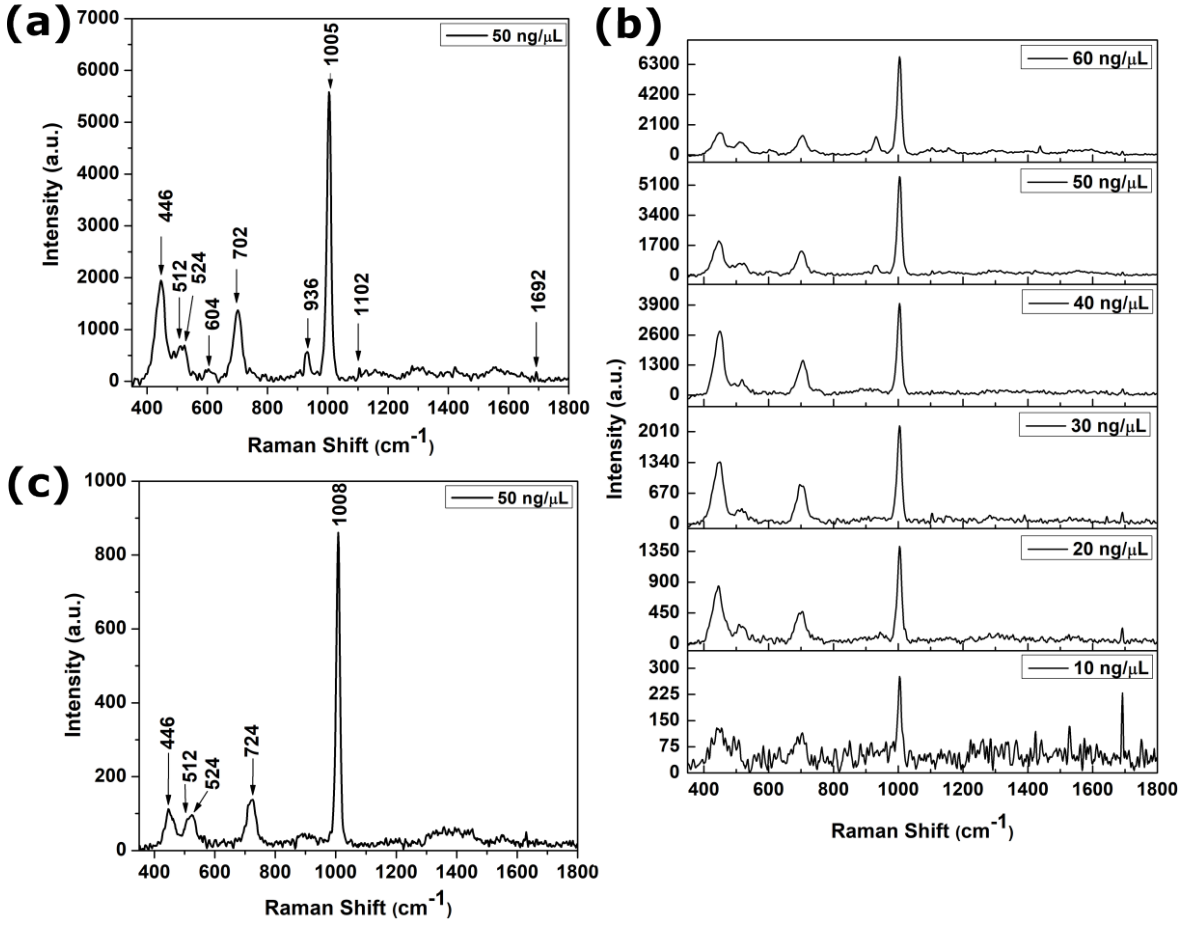

Figure 5.8: (a) SERS spectrum of rotavirus RNA of concentration 50 ng/µL collected from AuNP decorated BR-DVD SERS substrate. (b) Variation of SERS signal intensities with concentrations of rotavirus RNA from 60 ng/µL to 10 ng/µL, and BR-DVD as SERS substrate. (c) SERS spectrum of rotavirus RNA of concentration 50 ng/µL collected from commercially available SERS substrate.

cytosine and uracil with phosphate backbone and carbon sugar. The characteristic Raman spectra for the individual nucleobases can be found elsewhere [14]. However, once these molecules combine to form the dsRNA, the signature Raman peaks of some of the molecules maybe perturbed or may disappear in the final Raman spectrum [15].

The detail extraction procedure of rotavirus RNA from clinical stool specimen has already been discussed in section 5.2.2. Six microliters of RNA solution of concentration 50 ng/µL is pipetted on the fabricated SERS substrate and allowed to dry for 1 hour before recording the Raman spectrum. Figure 5.8(a) represent the characteristic Raman peaks of the RNA sample of concentration 50 ng/µL. Distinct Raman peaks have been observed at 446 cm^{-1}, 512 cm^{-1}, 604 cm^{-1}, 702 cm^{-1} and 1005 cm^{-1} in the characteristic spectrum. Chemical structure of nucleobases in RNA are depicted in the Figure 5.7. The signature Raman peaks at 446 cm^{-1} and 604 cm^{-1} are attributed to out-of-plane ring torsion and in-plane ring deformation vibration of cytosine molecule present in the sample [16]. Raman peak at 702 cm^{-1} is attributed to ring breathing mode of adenine molecule [17]. Again, the Raman peak at 512 cm^{-1} is attribute to the guanine molecule ring deformation [14]. Sharp peaks at 1005 cm^{-1} is arising due to the stretching vibration of aromatic ring present in the sample [18, 19]. The weak peaks at 1102 cm^{-1} and 1692 cm^{-1} are attribute to PO_2^- symmetric stretching and C=O stretching of uracil, respectively [20].

In the next step, different concentrations of RNAs ranging from 60 ng/µL to 10 ng/µL have been detected with the designed substrate. RNA sample solutions of concentration 10, 20, 30 40, 50 and 60 ng/µL have been prepared, and 6 µL each of the sample solution has been pipetted on the fabricated SERS substrate and allowed to dry for 1 hour in vacuum desiccator. Figure 5.8(b) depicts the SERS spectra of six concentrations of RNAs. The characteristic peak intensity increases gradually with concentration from 10 ng/µL till 40 ng/µL. After this concentration, significant change in the peak intensities can be observed. The intensity of the peaks 446 cm^{-1} and 702 cm^{-1} are observed to be decreased with the increase in concentration. This results indicate that the designed SERS substrate is suitable for monitoring the fingerprint of the biological samples in the laboratory environment.

5.3.4 SERS spectra of rotavirus RNA collected from the SERSitive SERS substrate

SERS spectrum of rotavirus RNA has also been recorded using commercially available SERS substrate from SERSitive, Warsaw, Poland. Six microliters of RNA solution of concentration 50 ng/µL is pipetted on the SERSitive SERS substrate and allowed to dry for 1 hour. Figure 5.8(c) represents the SERS spectra of rotavirus RNA collected from SERSitive SERS substrate. It has been observed that there is no shift in the peaks

of cytosine at 446 cm^{-1} and guanine at 512 cm^{-1}. However, for adenine molecule, the signature Raman peak at 724 cm^{-1} is shifted to 702 cm^{-1} when SERS spectra of rotavirus RNAs are collected using BR-DVD SERS substrate [17]. It is further noticed that a shift of 3 cm^{-1} has occurred corresponding to the peak position at 1008 cm^{-1} when the scattered signals of the same RNA samples were recorded from the BR-DVD substrate. These shifts in the peak positions are attributed to the use of citrate-capped AuNPs for the development of BR-DVD SERS substrate [21].

Owing to the use of relatively smaller dimension nanoparticles for the development of the SERS substrates, the number of hot-spot regions per unit area will be more compared to the metal nanoparticle decorated BR-DVD SERS substrates developed by Chamuah et al. [2] and Ngamaroonchote et al. [22]. To trap RNAs in the narrow hot-spot regions, nanoparticles of smaller dimension are preferred over larger size nanostructures. In our case, although with smaller NPs the magnitude of the coupled LSPR field was moderate, the higher density of hot-spots over the sensing region of the substrate yields a good degree of reproducibility. Our experimental results as shown in figure 5.6(c) validates this claim. The overall cost involved to fabricate the proposed SERS substrate is relatively low, INR 16 ($\sim$ \$0.2), and the fabrication process is relatively simple.

5.4 Summary

In summary, a highly reproducible SERS substrate has been fabricated by trapping AuNPs of diameter 23 nm in the nanochannels of the BR-DVD substrate. The usability of the designed SERS substrate was further investigated by detecting the Raman spectra of rotavirus RNA in the laboratory environment. The cost involved in designing the substrate is very low, INR 16 ($\sim$ \$0.2) per substrate, and can be used as a disposable SERS substrate. The proposed SERS substrate could emerge as a highly reproducible platform for other SERS-based sensing studieds in the laboratory environment.

Bibliography

[1] Nieuwoudt, M. K., Martin, J. W., Oosterbeek, R. N., Novikova, N. I., Wang, X., Malmström, J., Williams, D. E., and Simpson, M. C. Gold-sputtered blu-ray discs: simple and inexpensive sers substrates for sensitive detection of melamine. *Analytical and bioanalytical chemistry*, 408:4403–4411, 2016.

[2] Chamuah, N., Saikia, A., Joseph, A. M., and Nath, P. Blu-ray dvd as sers sub-

strate for reliable detection of albumin, creatinine and urea in urine. *Sensors and Actuators B: Chemical*, 285:108–115, 2019.

[3] Gautam, R., Lyde, F., Esona, M. D., Quaye, O., and Bowen, M. D. Comparison of premier™ rotaclone®, prospect™, and ridascreen® rotavirus enzyme immunoassay kits for detection of rotavirus antigen in stool specimens. *Journal of Clinical Virology*, 58(1):292–294, 2013.

[4] Organization, W. H. et al. Manual of rotavirus detection and characterization methods. Technical report, World Health Organization, 2009.

[5] Multiphysics, C. Introduction to comsol multiphysics®. *COMSOL Multiphysics, Burlington, MA, accessed Feb*, 9(2018):32, 1998.

[6] Chamuah, N., Chetia, L., Zahan, N., Dutta, S., Ahmed, G. A., and Nath, P. A naturally occurring diatom frustule as a sers substrate for the detection and quantification of chemicals. *Journal of Physics D: Applied Physics*, 50(17):175103, 2017.

[7] Kim, A., Ou, F. S., Ohlberg, D. A., Hu, M., Williams, R. S., and Li, Z. Study of molecular trapping inside gold nanofinger arrays on surface-enhanced raman substrates. *Journal of the American Chemical Society*, 133(21):8234–8239, 2011.

[8] Wu, K., Li, T., Schmidt, M. S., Rindzevicius, T., Boisen, A., and Ndoni, S. Gold nanoparticles sliding on recyclable nanohoodoos—engineered for surface-enhanced raman spectroscopy. *Advanced Functional Materials*, 28(2):1704818, 2018.

[9] Zhuang, Z., Shi, X., Chen, Y., and Zuo, M. Surface-enhanced raman scattering of trans-1, 2-bis (4-pyridyl)-ethylene on silver by theory calculations. *Spectrochimica Acta Part A: Molecular and Biomolecular Spectroscopy*, 79(5):1593–1599, 2011.

[10] Kumar, P., Khosla, R., Soni, M., Deva, D., and Sharma, S. K. A highly sensitive, flexible sers sensor for malachite green detection based on ag decorated microstructured pdms substrate fabricated from taro leaf as template. *Sensors and Actuators B: Chemical*, 246:477–486, 2017.

[11] Pu, H., Zhu, H., Xu, F., and Sun, D.-W. Development of core-satellite-shell structured mnp@ au@ mil-100 (fe) substrates for surface-enhanced raman spectroscopy and their applications in trace level determination of malachite green in prawn. *Journal of Raman Spectroscopy*, 53(4):682–693, 2022.

[12] He, L., Kim, N.-J., Li, H., Hu, Z., and Lin, M. Use of a fractal-like gold nanostructure in surface-enhanced raman spectroscopy for detection of selected food contaminants. *Journal of agricultural and food chemistry*, 56(21):9843–9847, 2008.

[13] Nguyen, A. H., Peters, E. A., and Schultz, Z. D. Bioanalytical applications of surface-enhanced raman spectroscopy: de novo molecular identification. *Reviews in analytical chemistry*, 36(4):20160037, 2017.

[14] De Gelder, J., De Gussem, K., Vandenabeele, P., and Moens, L. Reference database of raman spectra of biological molecules. *Journal of Raman Spectroscopy: An International Journal for Original Work in all Aspects of Raman Spectroscopy, Including Higher Order Processes, and also Brillouin and Rayleigh Scattering*, 38 (9):1133–1147, 2007.

[15] Badr, Y. and Mahmoud, M. Effect of silver nanowires on the surface-enhanced raman spectra (sers) of the rna bases. *Spectrochimica Acta Part A: Molecular and Biomolecular Spectroscopy*, 63(3):639–645, 2006.

[16] Morla-Folch, J., Xie, H.-n., Alvarez-Puebla, R. A., and Guerrini, L. Fast optical chemical and structural classification of rna. *Acs Nano*, 10(2):2834–2842, 2016.

[17] Muniz-Miranda, M., Gellini, C., Pagliai, M., Innocenti, M., Salvi, P. R., and Schettino, V. Sers and computational studies on microrna chains adsorbed on silver surfaces. *The Journal of Physical Chemistry C*, 114(32):13730–13735, 2010.

[18] Zheng, W., Zhang, S., Gu, Y., Gong, F., Kong, L., Lu, G., Lin, G., Liang, B., and Hu, L. Non-invasive metabolomic profiling of embryo culture medium using raman spectroscopy with deep learning model predicts the blastocyst development potential of embryos. *Frontiers in Physiology*, 12:777259, 2021.

[19] Chen, Y., Chen, G., Feng, S., Pan, J., Zheng, X., Su, Y., Chen, Y., Huang, Z., Lin, X., Lan, F., et al. Label-free serum ribonucleic acid analysis for colorectal cancer detection by surface-enhanced raman spectroscopy and multivariate analysis. *Journal of biomedical optics*, 17(6):067003–067003, 2012.

[20] Benevides, J. M., Tsuboi, M., Bamford, J., and Thomas, G. Polarized raman spectroscopy of double-stranded rna from bacteriophage phi6: local raman tensors of base and backbone vibrations. *Biophysical journal*, 72(6):2748–2762, 1997.

[21] Kneipp, K., Haka, A. S., Kneipp, H., Badizadegan, K., Yoshizawa, N., Boone, C., Shafer-Peltier, K. E., Motz, J. T., Dasari, R. R., and Feld, M. S. Surface-enhanced raman spectroscopy in single living cells using gold nanoparticles. *Applied Spectroscopy*, 56(2):150–154, 2002.

[22] Ngamaroonchote, A. and Karn-Orachai, K. Bimetallic au–ag on a patterned substrate derived from discarded blu-ray discs: Simple, inexpensive, stable, and reproducible surface-enhanced raman scattering substrates. *Langmuir*, 37(24):7392–7404, 2021.